

# Shear Lag in Truss Core Sandwich Beams

by

Ryan Roberts

Submitted to the Department of Mechanical Engineering in Partial Fulfillment  
of the Requirements for the Degree of

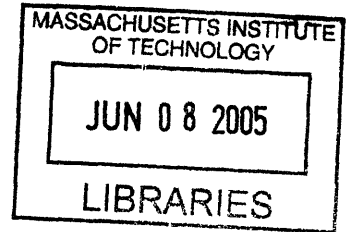
Bachelor of Science

at the

Massachusetts Institute of Technology

June 2005

© 2005 Ryan Roberts  
All rights reserved



The author hereby grants to MIT permission to reproduce and to distribute publicly paper and electronic copies of this thesis document in whole or in part.

Signature of Author.....  
Department of Mechanical Engineering  
May 6, 2005

Certified by.....  
Lorna J. Gibson  
Matoula S. Salapatas Professor of Materials Science and Engineering  
Professor of Mechanical Engineering  
Professor of Civil Engineering  
Thesis Supervisor

Accepted by.....  
Professor Ernest G. Cravalho  
Chairman, Undergraduate Thesis Committee

**ARCHIVES**

# Shear Lag in Truss Core Sandwich Beams

by

Ryan Roberts

Submitted to the department of Mechanical Engineering  
on May 6, 2005 in Partial Fulfillment of the  
Requirements for the Degree of Bachelor of Science in  
Mechanical Engineering

## ABSTRACT

An experimental study was conducted to investigate the possible influence of shear lag in the discrepancy between the theoretical and measured stiffness of truss core sandwich beams. In previous studies, the measured values of stiffness in loading have proven to be 50% of the theoretical stiffness during three point bending tests. To test the effect of shear lag on this phenomenon, the beams' dimensions were altered to decrease the presence of shear lag in a gradual manner so a trend could be observed.

The experimental trials were carried out on three types of beams each with different diameters of truss material. Results show that this study has improved the accuracy of the measured results from previous studies with the two smallest truss diameter beams. Because the discrepancy between the theoretical and measured values is the greatest for the largest beams, (when the shear deflection has the least influence), it is concluded that shear lag is not responsible for the discrepancy between measured and theoretical stiffness.

Thesis Supervisor: Lorna J. Gibson

Title: Matoula S. Salapatas Professor of Materials Science and Engineering, Professor of Mechanical Engineering, Professor of Civil Engineering

## 1. Introduction

In order to create structures with a high specific stiffness, sandwich designs have been investigated. These materials are composed of a face material and a low-density core. Previous research into high specific strength and stiffness sandwich structures has involved honeycomb and foams as the core materials.

Metallic honeycomb is a two-dimensional repeating structure seen below in Fig. 1.

Because the honeycomb structure has closed cells it does not lend itself to multifunctional applications such as heat transfer, which requires flow through cells. The face sheets of the sandwich beam are also usually bonded to the core by some type of adhesive. The use of adhesive to bond the face sheets makes these structures subject to moisture related degradation and delamination.

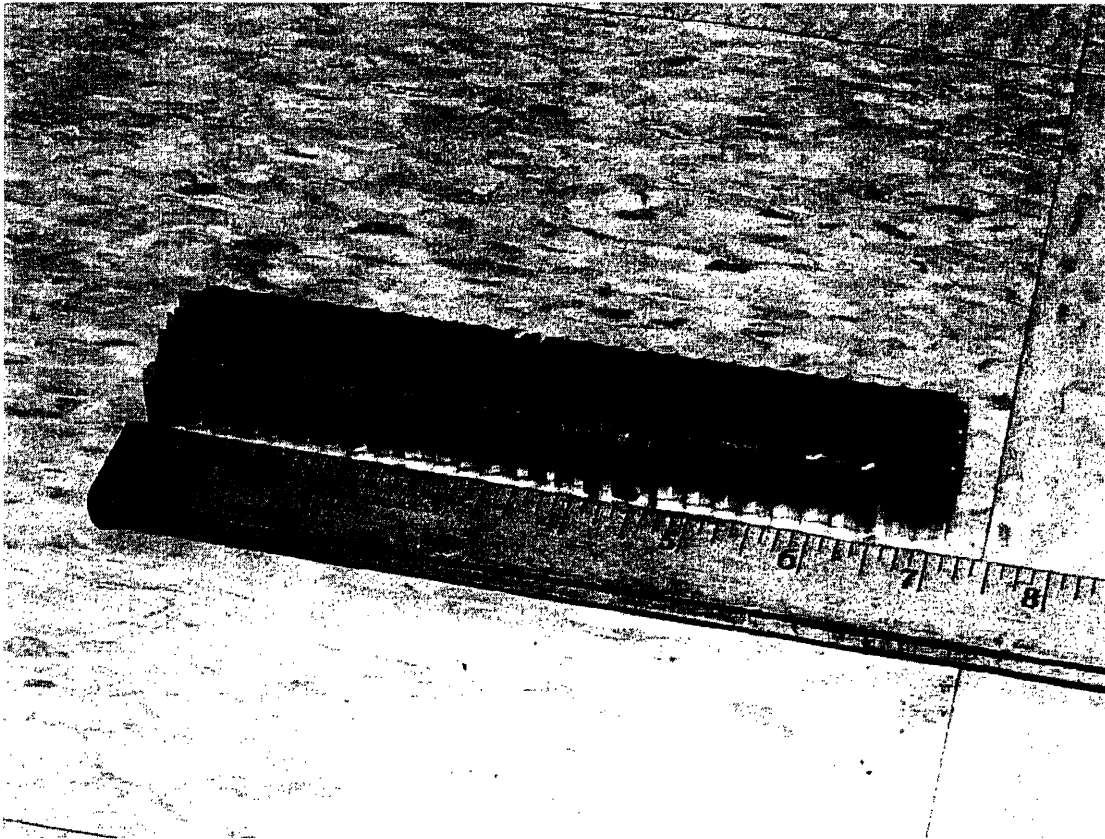


**Figure 1: Aluminum honeycomb core material.**

The other low-density core material, foam, seen below in Fig.2 is often made by infusing bubbles into molten metal. This leads to irregularities in cell orientation, shape and size, as well as variations in density within the material. This in turn causes difficulty in modeling the mechanical behavior in a heterogeneous material. Because of the nature of the structure, loads are supported by bending in the cell walls and this is not an efficient use of mass. Due to defects in the cell structure and inhomogeneities in density, metal foam-core sandwich structures are not as efficient as theoretically possible.

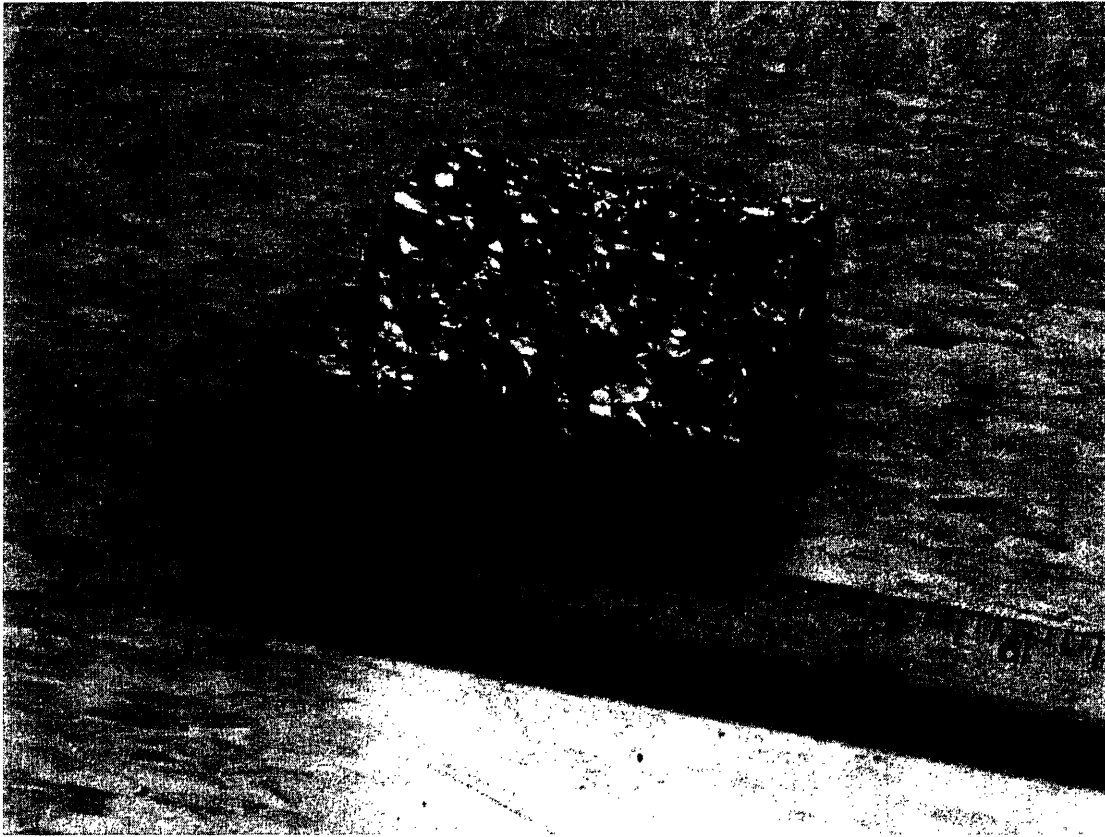


**Figure 2: Aluminum foam core material.**

Applications for sandwich structures involve designs where weight is important, such as in aircraft construction or auto racing. Other products that make use of sandwich panels include helicopter rotor blades, building construction, sporting equipment and the interiors of ships and trains (Wallach 2004). For impact absorption purposes honeycombs have been widely used in car bumpers. In structural applications, truss core beams have greater potential because the structure is more optimally designed by allowing the stresses in the core to be transmitted uniaxially along the truss members.

The current investigation is concerned with a steel truss core design. Previous research has proven that the performance of this design is equal to or superior to that of

honeycomb, foam or open cell sandwich structures (Wallach and Gibson 2001). In addition to the mechanical properties being optimized, the welded joints provide a more durable alternative to adhesives, which are liable to delamination, moisture damage, limitations in the temperature range over which they can be used (Wallach 2004). A unique benefit of the truss core beam is its ability to serve multifunctional purposes. With the truss design, the sandwich structure can simultaneously support mechanical loads as well as perform acoustic damping and heat-transfer functions by flowing coolant through the core, unlike foams or honeycombs (Queheillalt, D.T. and Wadley H.N.G. 2005).

Though the truss core design has proven versatile and mechanically promising, experimental measurements of stiffness tend to lie below those obtained theoretically. In previous analysis the shear component of the stiffness calculation was low by 300% on average and the total measured stiffness was only 20 to 50% of the theoretical value (Wallach 2004). One hypothesis is that this discrepancy arises in the shear component of the stiffness calculation as a result of shear lag, a non-uniform stress field in the longitudinal direction of the beam. In this case there are high stress peaks at the welded joints and low stress sections between these joints. The magnitude of this phenomenon can be controlled through changing the geometry of the beams. In this study, beams of longer total length and of three different core stiffnesses were created to detect the possible influence of this phenomenon on truss beams.

## 2. Literature Review

Sandwich plates with truss cores and solid sheet faces can be optimally designed for a high specific stiffness in applications necessitating combinations of bending and transverse shear loads (Wicks and Hutchinson 2001). These truss core beams compare favorably with beams composed of honeycomb and are significantly lighter than the competing design using metallic foam cores (Deshpande and Fleck 2001). The design of the truss core induces axial forces in the individual truss members, which leads to a high specific stiffness and strength (Wallach and Gibson 2001). In addition to the superior mechanical characteristics, the cavity between the face sheets can be used to store liquid or compressed air for heat transfer purposes (Wicks and Hutchinson 2001).

The construction of the truss core can be achieved in multiple ways. In the casting method, a negative for the truss core can be manufactured via injection molding or stereo lithography. This requires fabricating the bottom and the top of this design separately and then combining them to form the full negative of the truss core. The truss core itself can then be manufactured by using the negative copy created in an investment casting process, where the original negative copy is burned away leaving the desired truss core. This type of truss core can be seen in Fig 3. With current technologies trusses can be created to the micron scale (Wallach and Gibson 2001).

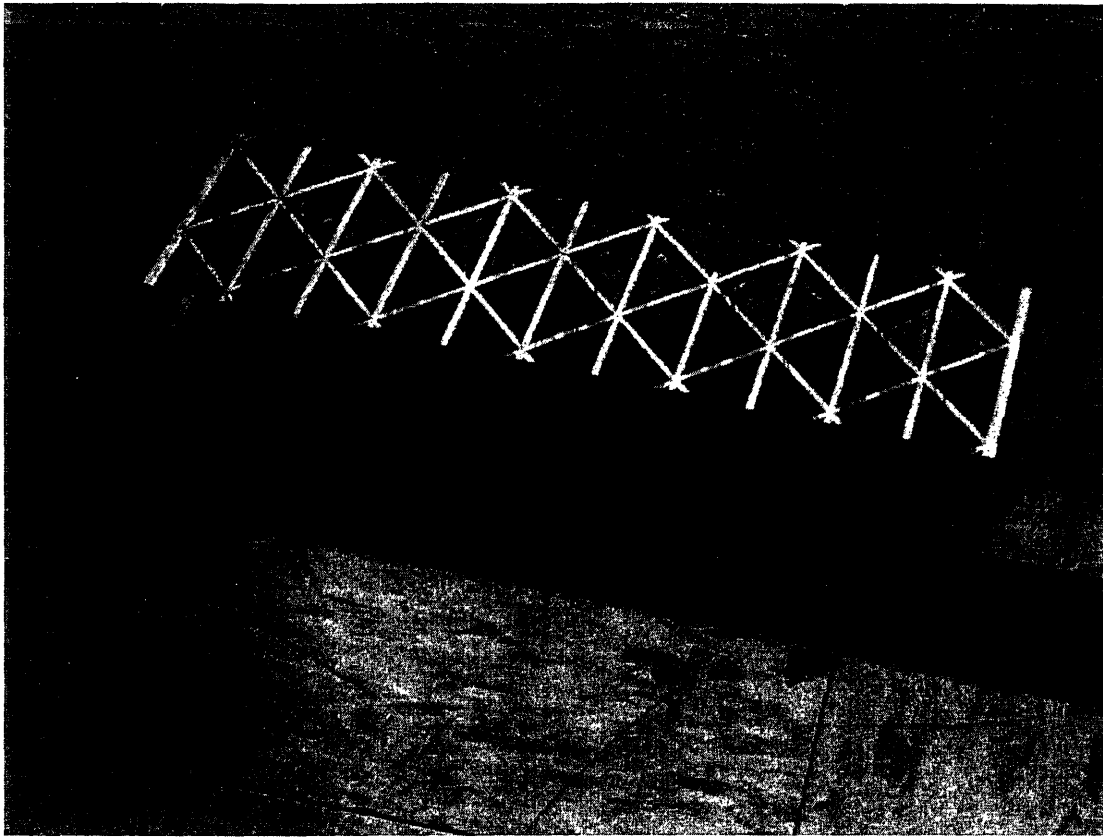


**Figure 3: Investment cast aluminum truss core.**

Another option is a combination of braising and electro-discharge machining (EDM). In this approach, straight rods are oriented with the help of a jig to form a lattice. These rods are then braised together. The process is repeated to manufacture multiple lattices which are then stacked and braised together. This stacked lattice structure, which can be varied in orientation to form different truss core geometries, forms the core of the beam. Once this structure has been braised together and allowed to cool, the raw core 3D lattice material is cut using EDM to exact specifications. This EDM cut core is then braised to the face sheets, which must be placed in the vacuum furnace. The end result is a truss sandwich beam (Queheillalt and Wadley 2005).

A third option which is used to make the beam in this experiment is a wire bending and welding technique. The core is made from wire of a certain thickness which is periodically bent at right angles. At the corners the face sheet is then resistance welded to the wire in a manner which yields the 3D truss structure as seen in Fig. 4 (Wallach 2004). When considering other forms of low-weight, high stiffness beams, the truss core design is superior, considering its resistance to delamination and moisture intrusion, its multifunctional capabilities, and its ease of manufacture (Wicks and Hutchinson 2004).

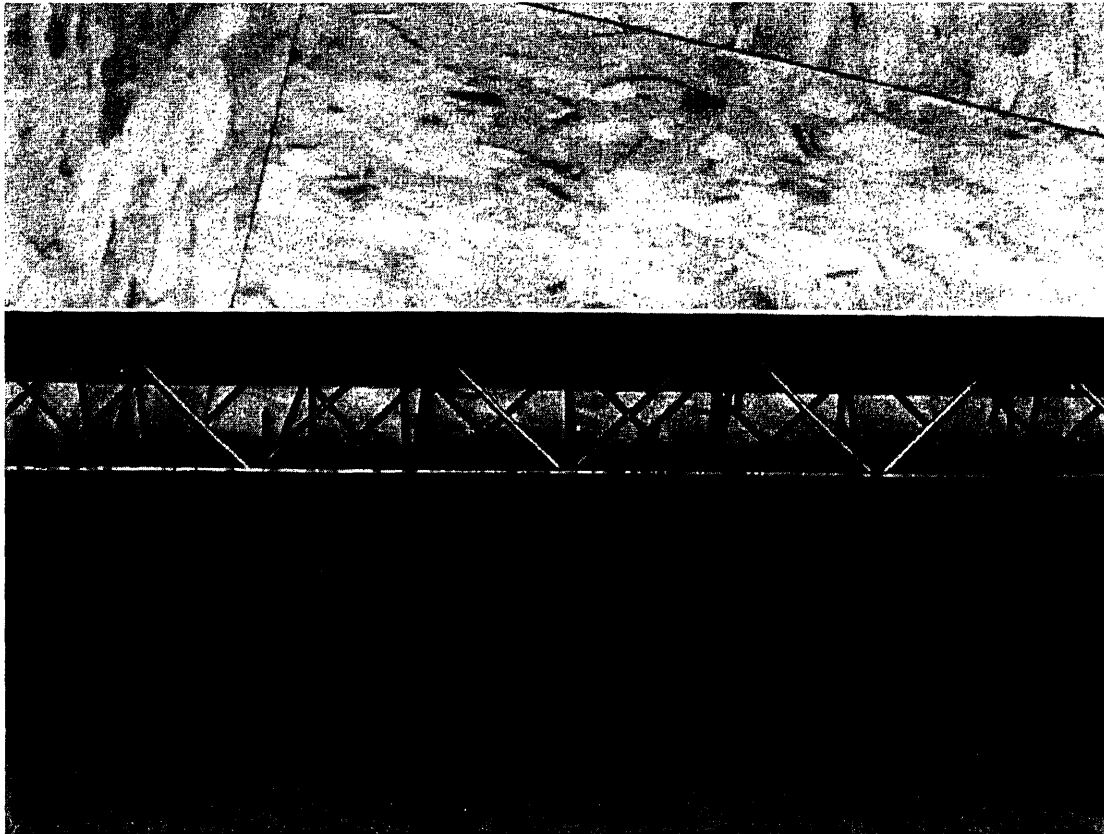


**Figure 4: Welded truss core sandwich beam of .5715 mm truss wire radius under consideration in this study.**

Mechanically the truss core beam is analogous to the “I-beam”. The face sheets of the truss beam are similar to the flanges of the I-beam and the truss core is similar to the web, the thin vertical portion of the I beam. The face sheets and the flanges carry most of the normal load, and most of the shear stress is carried by the trusses and the vertical part of the I beam. Because of the truss geometry, the shear is carried by alternating axial tensile and compressive loads in the individual members. The mechanical properties of the beam depend on the geometry and density of the core, the thickness of the face sheets and the panel as a whole. In modeling the mechanics of the truss core beam it has been shown that assuming the truss core joints to be pinned joints is adequate though it ignores the contribution of bending moments in the welded joints (Deshpande and Fleck 2001, Wallach and Gibson 2001).

The elastic deformation at the measured mid-span point is the sum of the flexural and shear deflections (Deshpande and Fleck 2001). Failure occurs through four competing modes of collapse: yielding of the sheet faces, buckling of the face sheets, indentation and core shear (Deshpande and Fleck 2001). In previous studies of a similar “octet” truss design, the measured stiffness was determined to be less than that of the theoretical value (Deshpande 2001). Wallach and Gibson have also observed similar results with the truss design investigated in this experiment. More current investigations of braised rod beams have returned unloading stiffness values slightly higher than theoretical values, though loading stiffness measurements which reflect a more realistic loading history are lower by a factor of two (Queheillalt and Wadley 2005).

There has also been a lack of investigation into variations of beam dimensions. Deshpande and Fleck noted that tests with different strut dimensions would be ideal but they were limited by their tools and technology (2001, 6291). One study has used variation in truss wire diameter (by about approximately 30%) (Chiras 2002). The peak load recorded for the largest diameter is roughly twice that of the smallest truss diameter but they do not numerically report the stiffness of the different beams or compare them in a clear manner visually. Though it has been recorded in multiple studies no investigation published thus far has studied the discrepancy between the theoretical and measured stiffness of the truss design or the possible influence of shear lag.

### 3. Theoretical Analysis

#### 3.1 Bending Stiffness

In order to arrive at the final stiffness for the truss sandwich beams in three point bending, the deflection is first written as the sum of the bending and shear displacements (Allen 1969):

$$\delta = \frac{FL^3}{48(EI)_{eq}} + \frac{FL}{4(AG)_{eq}} \quad (1)$$

where

$$(EI)_{eq} = \frac{E_f bt^3}{6} + \frac{E_f btd^2}{2} + \frac{E_c bc^3}{12} \approx \frac{E_f btd^2}{2} \quad (2)$$

and

$$(AG)_{eq} = \frac{bc^2}{c} G_{13} \approx bcG_{13} \quad (\text{Deshpande and Fleck 2001}). \quad (3)$$

In this equation, the shear modulus of the truss core is (Deshpande and Fleck 2001)

$$G_{13} = E_s \frac{\bar{\rho}}{8} \sin^2 2\omega \quad (4)$$

where the core relative density is (Deshpande and Fleck 2001)

$$\bar{\rho} = \frac{2\pi}{\cos^2(\omega)\sin(\omega)} \left(\frac{a}{l}\right)^2 \quad (5)$$

This finally arrives at

$$\frac{\delta}{F} = \frac{L^3}{24E_f b t d^2} + \frac{2L}{bcE_s \bar{\rho} \sin^2(2\omega)} \quad (6)$$

where the reciprocal

$$\frac{F}{\delta} = \frac{1}{\frac{\delta}{F}} \quad (7)$$

gives the stiffness in (Allen 1969).

### 3.2 Shear Lag

Shear lag depends on both the geometry and the material properties of the beam. For a beam with two flanges stiffened by regularly spaced webs, the shear lag decreases with the stiffness parameter  $m$  (Hildebrande, 1943):

$$m = \frac{3I_{web} + I_{flange}}{I_{web} + I_{flange}} \quad (8)$$

where  $I_{web}$  and  $I_{flange}$  are the moments of inertia of the web and flanges, respectively.

Shear lag also depends on the material properties through the parameter (Hildebrand, 1943)

$$n = \sqrt{\frac{27E}{32G} \frac{b}{L}} \quad (9)$$

where E is the Young's modulus of the flange and G is the shear modulus of the web, and b and L are the width and length of the beam.

For the truss core beam, the effective shear modulus of the core is

$$G_{truss} = \frac{\pi}{4} \frac{a}{l} \tan \omega \quad (10)$$

where  $\omega$  is the angle between the horizontal and the inclined truss wire. The corresponding effective moment of inertia of the truss core is then

$$I_{truss} = \frac{2a(l \sin \omega)^3}{12} \quad (11)$$

Shear lag decreases as m increases and as n decreases (Hildebrand, 1943). Increasing the diameter of the truss wire decreases shear lag through increasing the effective moment of inertia of the truss core (increasing m) and increasing the shear modulus of the core (decreasing n).

## 4. Method

### 4.1 Material

The sandwich beams in consideration are composed of steel wire (302 alloy) and steel sheet metal (304 alloy). Seen below in Fig.5 is a welded truss beam studied by Wallach and Gibson.

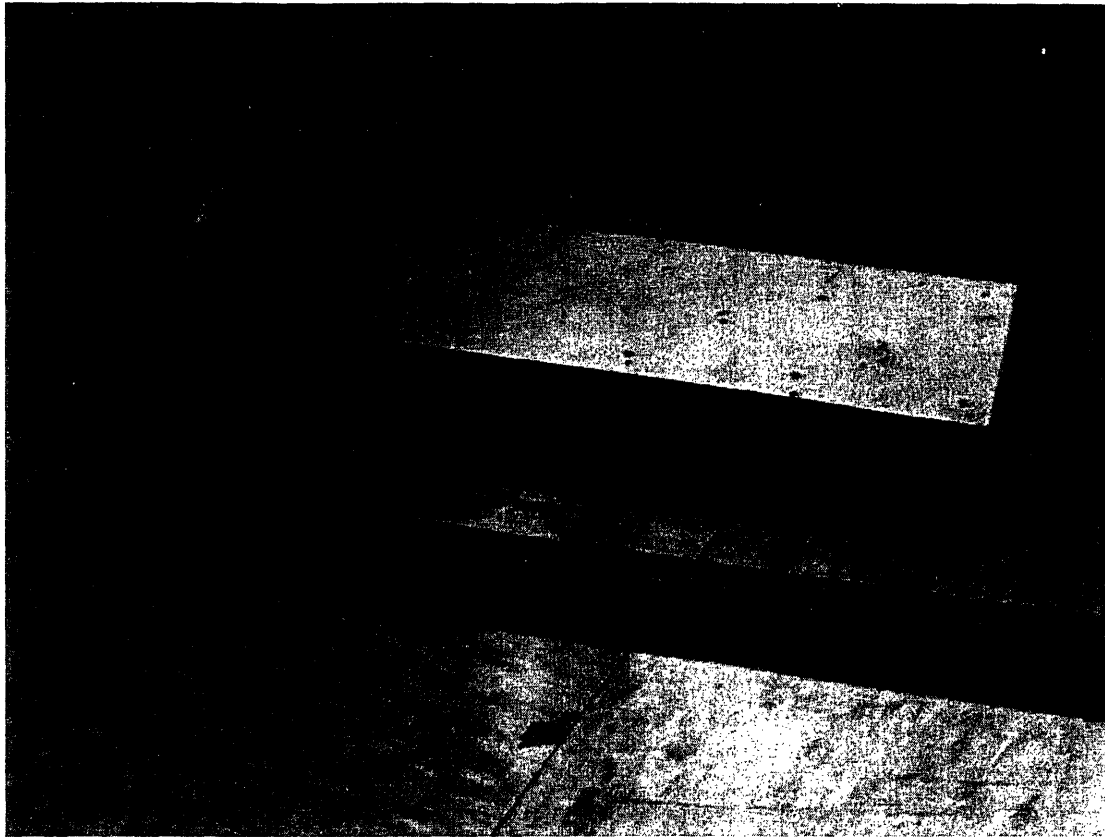


**Figure 5: Wallach and Gibson welded truss core beam with original shorter dimensions and small wire core thickness.**

The new beams in this study have an overall length extended to 30 inches from 11 inches and two larger core strut diameters in addition to the original size of the Wallach and Gibson beams, which is the smallest in this study. The diameter of the core truss material is .045, .086, and .176 inches for the small, medium and large wire thicknesses respectively. These wires, bent by Anchor Springs Inc. (Anaheim, CA), are fixed to the sheet steel face (0.028 inches thick) (McMaster Carr, Dayton, NJ) by electrode spot welding. The welding was done with 20 inch copper welding tongs on a Miller wt-2508 machine (Appleton, WI). One of the tongs seen below in Fig. 6 is specially designed to meet with the 45 degree bend of the core material. A schematic showing the beam geometry, is given in Fig. 7.

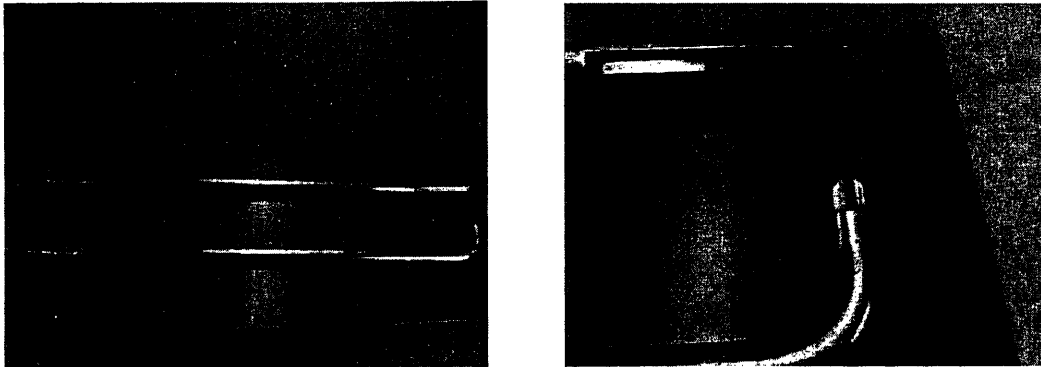


Figure 6: Custom made welding tong to fit the bend of the truss core material.

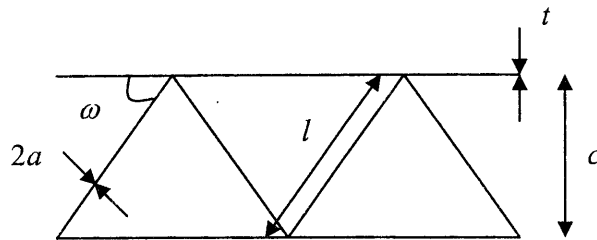


Figure 7: Truss core beam dimensions.

The final beam dimensions and characteristics are listed below in Tables 1 through 4.

Table 1: Truss core dimensions.

Beam type	Truss radius, $a$ (mm)	Truss angle, $\omega$ radians	Truss unit length, $l$ (mm)	Core height, $c$ (mm)
Small	0.5715	0.785	36.04	26.59
Medium	1.0922	0.741	34.44	26.11
Large	2.235	0.723	37.87	27.05

Table 2: Theoretical core mechanical properties.

Beam type	Core relative density, $\bar{\rho}$ (eqn 5)	Core shear modulus, $G_{13}$ (eqn 4) (Gpa)
Small	0.0045	0.1061
Medium	0.0172	0.4055
Large	0.0589	1.3755

**Table 3: Face sheet dimensions and mechanical properties.**

<b>Beam type</b>	<b>Face sheet thickness, <math>t</math></b> (mm)	<b>Young's Modulus, <math>E</math></b> (Gpa)	<b>Yield Stress, <math>\sigma_y</math></b> (MPa)
<b>Small</b>	0.711	190	205
<b>Medium</b>	0.711	190	205
<b>Large</b>	0.711	190	205

**Table 4: Total beam dimensions and mechanical properties.**

<b>Beam type</b>	<b>Beam Length, <math>L</math></b> (mm)	<b>Beam depth, <math>b</math></b> (mm)	<b>Theoretical Beam Stiffness (eqns 6,7)</b> (kN/mm)
<b>Small</b>	736.6	76	.3295
<b>Medium</b>	736.6	76	.4027
<b>Large</b>	736.6	88.9	.5392

The overall beam dimensions were chosen to be compatible with the limits set out by ASTM and to increase the aspect ratio to near 10:1 (ASTM C393).

Though there are many possibilities for the material used in the truss core sandwich beams, such as aluminum, titanium and rubber, steel was chosen for this investigation.

Other core materials can be seen below in Fig. 8.

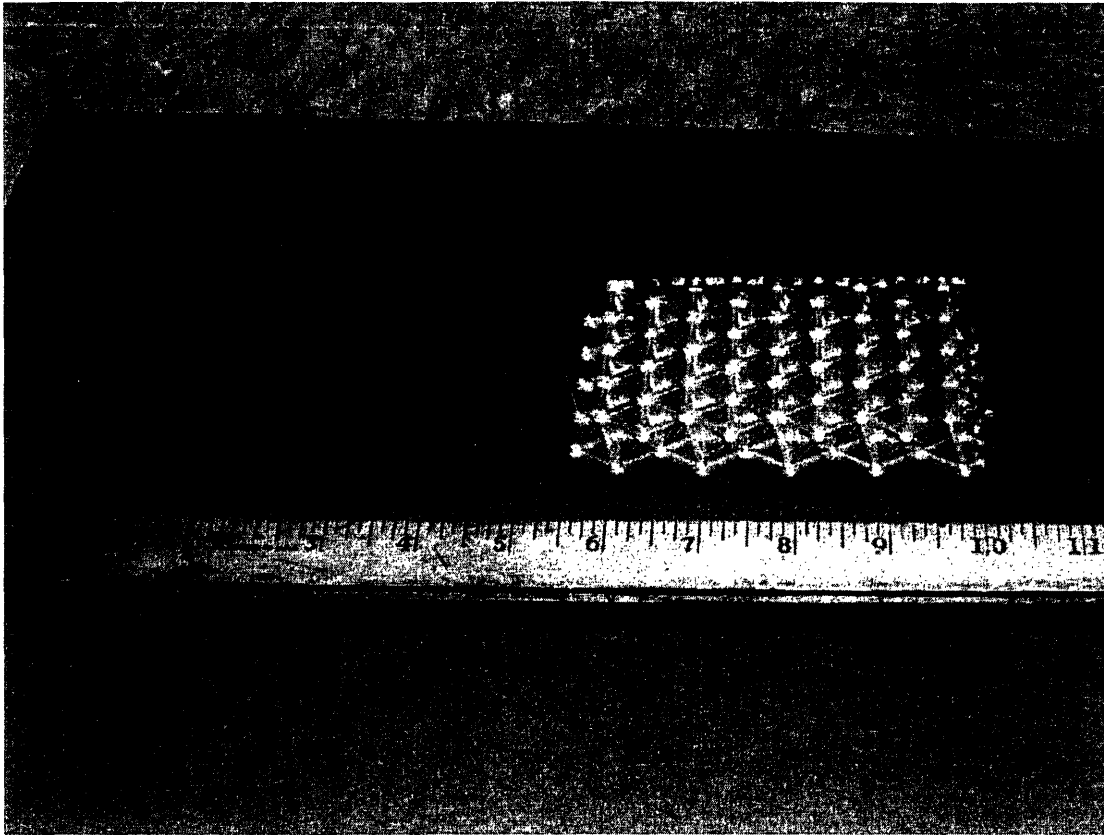


**Figure 8: Rubber and plastic core material of different dimensions.**

All metals have the capability of resistance welding, but for the purposes of this investigation, the ease of resistance welding of steel, and the relative cheapness of steel compared with other metals, made steel the most attractive choice (Wallach 2004).

## **4.2 Experimental Apparatus**

In order to measure the mid-span deflection of the beam in three point bending, a Trans-TEK 0241-00000 (Ellington, CT) LVDT with a measurement range of 3.75 mm and an precision of .5% was used. The testing setup can be seen below in Fig 9.

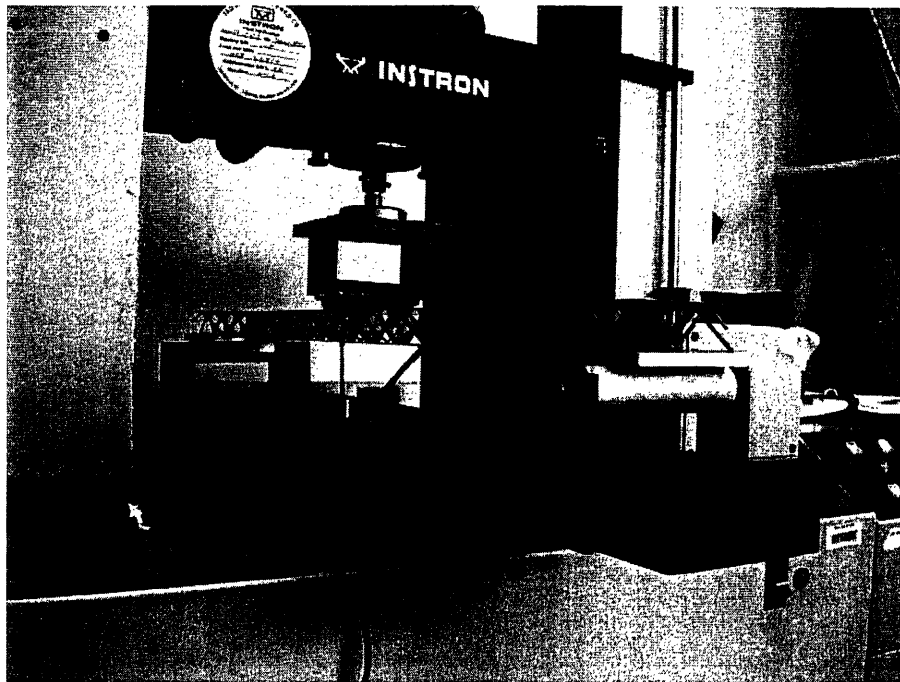


**Figure 9: Three point bending testing setup with medium wire thickness beam in place.**

The LVDT was calibrated before the testing process using a clamp and micrometer designed for this process. A computer acquisition system records the reading of the LVDT and the load from the load cell 5 times a second. The load cell used was a 1.5 kN load cell which was determined to be satisfactory by theoretically extrapolating the predicted load to the displacement where failure occurs. The three point apparatus seen here is custom made to test the unusually long specimens on this smaller Instron (model 4201, Norwood, MA). It is made of a steel channel and four “L” brackets. The rollers are of 1 inch diameter, aluminum supported by steel dowels of .375 inch diameter.

### **4.3 Specimen Preparation**

To make the faces, large sheets of metal were ordered from McMaster Carr and cut to size using a “guillotine” metal shearing machine. For the truss members running

lengthwise along the beam three pieces of wire bent by Anchor Springs were used. To make the shorter horizontal members, the long pieces of core material were cut down to the size of a one-unit truss using bolt shears (Fig. 10).



**Figure 10: A horizontal truss member.**

One beam requires three full size core pieces, 30 horizontal small pieces cut to size, and two pieces of sheet metal. The raw components of the beam are seen below in Fig 11.



**Figure 11: From the top: the largest steel core material made by Anchor Springs, medium diameter core material, smallest diameter core material, sheet metal cut to size for beam faces.**

#### **4.4 Load**

In order to measure the response of the truss core beams, they were subjected to monotonic loading in three point bending. An Instron model 4201 was used in conjunction with LabVIEW (National Instruments Inc., Austin, TX) software. The load was applied in the negative y direction on the top part of the beam over truss contact points with a roller of 1 inch diameter.

## **4.5 Experimental Procedure**

Before the tests, the LVDT and the load cell were calibrated. During the experiment the behavior of the beams were recorded. The specimens were labeled by number and photographs were taken during the testing process. Also, during the testing process specific notes were taken recording the sequence of events such as weld failure and face wrinkling.

## **4.6 Obtaining Results from data**

The data acquisition program outputs the load and mid-span displacement into a text file which was then imported into an Excel file for each beam. The maximum load was then determined by locating the maximum load in the testing sequence. The bending stiffness was calculated using the slope of the elastic portion of the curve before any yielding is noticeable. Care was taken to measure the stiffness of the loading curve before any weld failure which is recognizable by sharp step load decreases.

# **5. Results**

## **5.1 Stiffness**

In order to measure the stiffness of the beams it was necessary to locate the linear, elastic part of the loading history. Load-deflection curves for the small, medium and large truss diameter beams are shown below in Figs. 11, 12, 13.

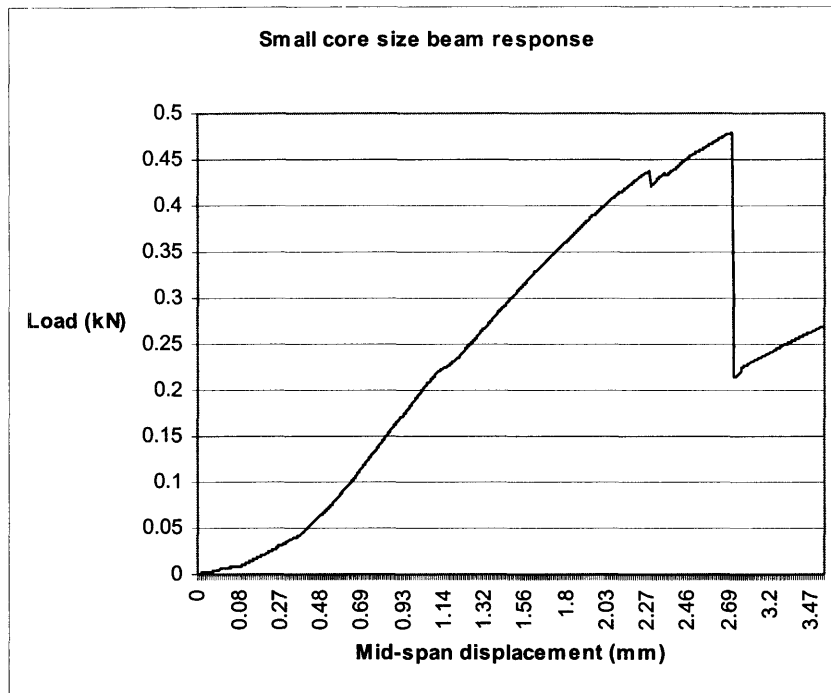


**Figure 11: Typical load-deflection curve for small truss core diameter beam.**

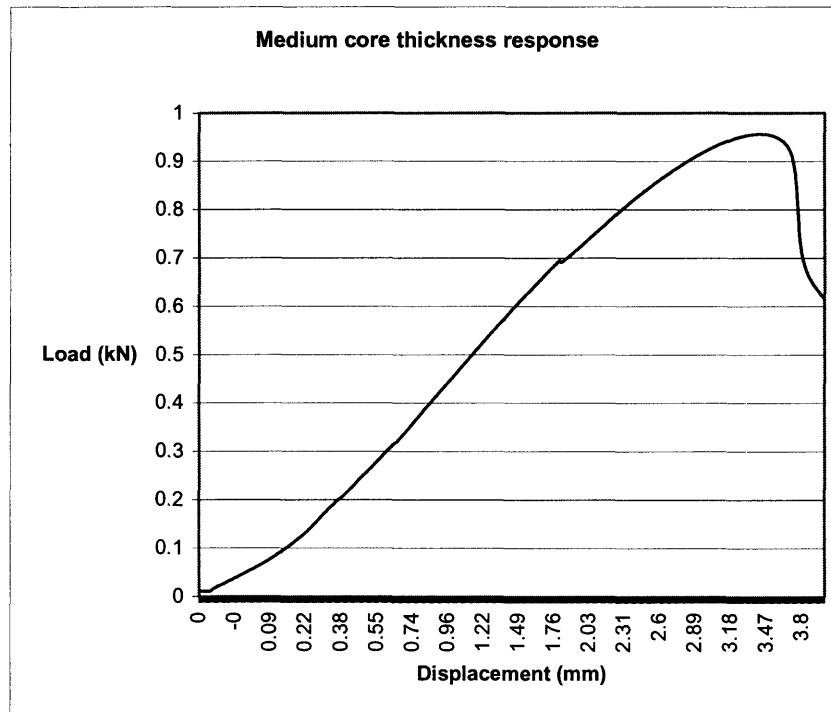


**Figure 12: Typical load-deflection curve for medium truss core diameter beam.**

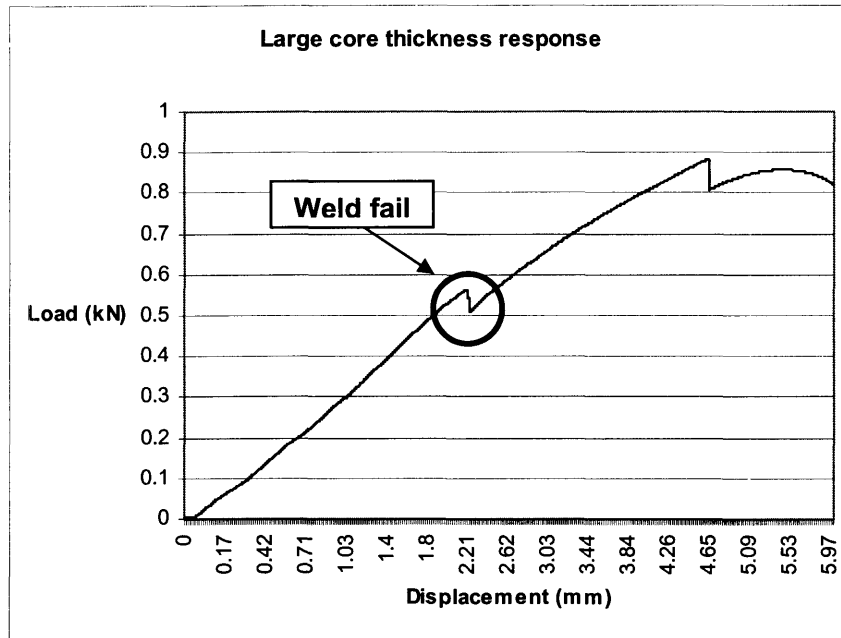
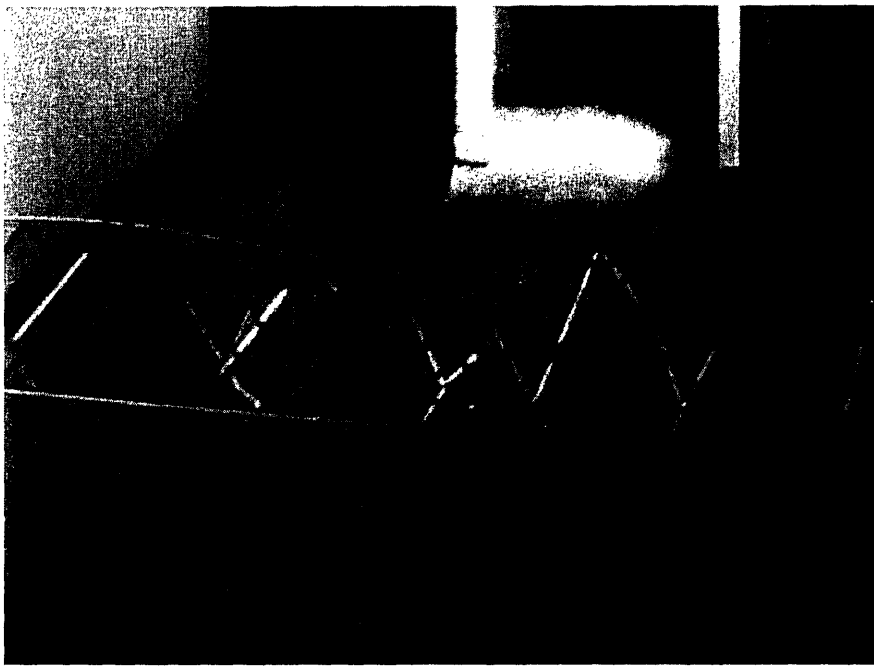


**Figure 13: Typical load-deflection curve for large truss core diameter beam.**

The curves displayed in these figures were selected from the experimental data to represent the average stiffness observed in each respective beam type. The remainder of the load-deflection curves for this study can be found in the Appendix.

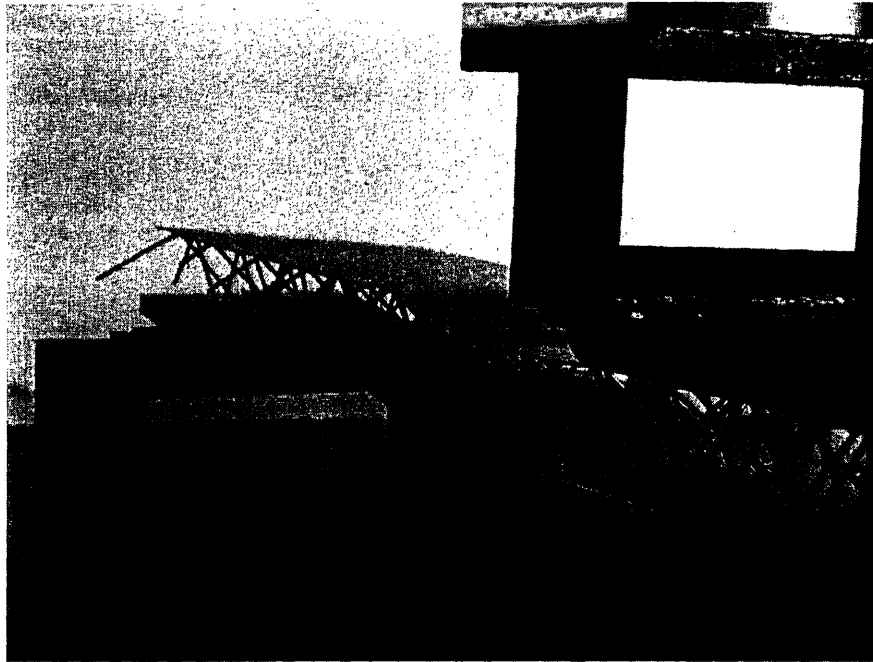
During the loading sequence most of the beams experienced weld failures which can be seen in both the linear and post-failure regimes of Figs 11, 12, and 13. Weld failure, which produces an audible “ping” noise corresponding to a load relaxation can be seen as a spike on the graph most clearly in the large diameter beam in Fig. 13. Though the curve remains nearly identical to that of the pre-weld failure curve, care was taken to measure the stiffness of the beams in the linear portion before any noticeable weld failure. After an initial linear-elastic regime initial failure is observed in either a major weld failure or a significant decrease in the slope of the curve. A rule such as the .2% yield stress may be used to obtain this value. The peak loads were simply taken from the maximum load sustained by the beams.

The observed mode of failure under the beams' peak load varied with the type of beams. For the small diameter truss beams, roughly half failed by core buckling and half failed by core shear. In the medium and large truss diameter beams the failure of the beams occurred at the faces in wrinkling. Photographs taken during the testing which depict different modes of failure can be seen below in Figs. 14, 15, and 16.



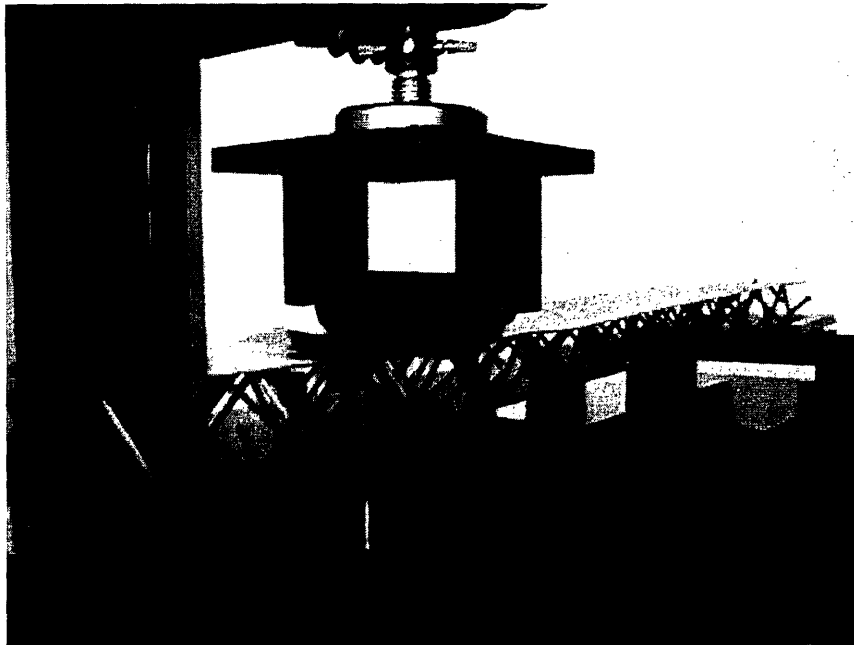
**Figure 14: Core failure by strut buckling in a small truss diameter beam.**

Fig. 14 depicts failure by the core which occurred only in the small diameter core beams. In this case the axial loads in the individual trusses caused plastic buckling which led to total beam collapse



**Figure 15: Total beam buckle caused by core shear failure between the mid-span load and end supports.**

In Fig. 15, a failure mechanism which was not anticipated by the theoretical calculations was observed. In this case, there were major truss failures between the mid-span and the support which led to total beam failure. This mode of failure was observed only in the small diameter truss core beams.



**Figure 16: Failure by face wrinkling in a medium truss diameter beam.**

Fig. 16 depicts the mode of failure which occurred in every large and medium truss diameter beam. These beams failed by face wrinkling in which the face sheets fail first by buckling near, but not under the mid-span loading point.

A comparison of the experimentally and theoretically obtained values for stiffness and peak load can be seen below in Tables 5, 6, 7, and 8.

**Table 5: Measured and theoretical beam stiffness for small truss diameters.**

Beam Number	Measured Stiffness (kN/mm)	Theoretical Stiffness (kN/mm)	Measured Percent	
			of Theoretical Stiffness %	Peak Load kN
1	0.25	0.3295	75.9	0.545
2	0.22	0.3295	66.8	0.357
3	0.3	0.3295	91.0	0.468
4	0.16	0.3295	48.6	0.501
5	0.21	0.3295	63.7	0.438
6	0.25	0.3295	75.9	0.694
7	0.24	0.3295	72.8	0.478
8	0.22	0.3295	66.8	0.518
9	0.25	0.3295	75.9	0.636

**Table 6: Measured and theoretical beam stiffness for medium truss diameters.**

Beam Number	Measured Stiffness (kN/mm)	Theoretical Stiffness (kN/mm)	Measured Percent	
			of Theoretical Stiffness %	Peak Load kN
3	0.26	0.362	71.8	0.987
4	0.38	0.362	105.0	0.872
5	0.37	0.362	102.2	0.957
7	0.26	0.362	71.8	1.02
8	0.19	0.362	52.5	0.943

**Table 7: Measured and theoretical beam stiffness for large truss diameters.**

Beam Number	Measured Stiffness (kN/mm)	Theoretical Stiffness (kN/mm)	Measured Percent	
			of Theoretical Stiffness %	Peak Load kN
1	0.21	0.5392	38.9	0.784
2	0.45	0.5392	83.5	0.986
3	0.26	0.5392	48.2	0.486
4	0.25	0.5392	46.4	0.795
5	0.26	0.5392	48.2	0.884
6	0.24	0.5392	44.5	0.741

**Table 8: Average measured and theoretical beam stiffness.**

<b>Core Size</b>	<b>Theoretical Stiffness (kN/mm)</b>	<b>Average Measured Stiffness (kN/mm)</b>	<b>Measured Stiffness Standard Deviation</b>	<b>Average Measured percent of Theoretical Stiffness</b>
<b>Small, 1.143mm core thickness beams</b>	0.3295	0.23	0.038	70.8
<b>Medium, 2.184mm core thickness beams</b>	0.4027	0.29	0.081	72.5
<b>Large, 4.47mm core thickness beams</b>	0.5392	0.29	0.086	50.0

During the testing a couple problems occurred which caused the data recorded during some trials to be thrown out. Often in the medium truss diameter beams, the beam would slide to one side or the other to relieve stress. This would place the loading roller over the face sheet with no truss weld beneath it, causing plastic deformation of the face sheet between the truss points. Because all the deformation is occurring in the face sheet this does not measure the desired properties of the beam as a whole and the results could not be used. Another problem that occurred a couple of times was that by chance the periodic truss structure would leave the end of the beam weakly supported with no weld joint. This caused large deformation in the face sheets at the end of the beam which again prevented the accurate measurement of the total beam response.

## **6. Discussion**

For all beam types tested in this study, the average measured stiffness was less than the theoretically predicted value, though the small and medium truss diameter beams measured closer to predicted values than in previous studies. The largest discrepancy

between the measured and calculated beam stiffnesses was observed in the beams with the largest diameter truss core. In the calculated beam stiffnesses, the shear deflection contributes a decreasing component of the total deflection as the truss core wire diameter increases (from 39% in the smallest diameter core to 3% in the largest diameter core). Because of this, it is unlikely that this phenomenon is associated with shear lag when the shearing component of the deflection is so small.

Another explanation for this (Chiras 2002) could be the increasing offset between the face sheet and the center of each connecting node in the truss core as the wire diameter increases. It has been suggested that this may cause discrepancies between measured and calculated results.

A possible improvement to the experimental technique used in this investigation would be to measure the unloading slope, as other studies (Chiras 2002) have found better agreement between the unloading slope and the theoretically predicted stiffness, though the loading slope is more relevant in practice.

## **7. Conclusion**

After analyzing the trends of the measured beam stiffnesses with those predicted theoretically, it is evident that shear lag does not account for the discrepancy between the measured and predicted beam stiffness. However, because of the trend in the results showing an increasing discrepancy between the measured and predicted values as the

wire truss diameter increases, it seems possible that this may be related to truss-face sheet offset phenomenon.

## References

- Allen, Howard G. (1969). "Analysis and Design of Structural Sandwich Panels." Pergamon Press, New York.
- ASTM Standard C393-00, (2000) Standard test method for shear properties of sandwich core materials. American Society for Testing and Materials.
- J.C. Wallach, L.J. Gibson (2001) / International Journal of Solids and Structures 38 7187-7196
- Queheillalt, D.T. and Wadley H.N.G. (2005) "Cellular metal lattices with hollow trusses". Acta Materialia 53 303-313.
- V.S. Deshpande et al. (2001) / J. Mech. Phys. Solids 49 1747-1769
- V.S. Deshpande, N.A. Fleck (2001) / International Journal of Solids and Structures 38 6725-6305
- Wallach, Jeremy. Notes (2004).
- Wallach, J.C. and Gibson L.J. (2001) "Defect sensitivity of a 3D truss material". Scripta Materialia 45 639-644.
- Wallach, J.C. (2004) "Manufacturing Truss Core Panels". Unpublished paper for Materials Processing, MIT.
- Wicks, Nathan and Hutchinson, J.W. "Optimal truss plates". International Journal of Solids and Structures". 38 (2001) 5165-5183.
- Wicks, Nathan and Hutchinson J.W. (2004) "Performance of sandwich plates with truss cores". Mechanics of Materials 36 739-751.

# Appendix

